Electronic Supplementary Material (ESI) for Dalton Transactions.

Supporting information

Synthesis and application of a water-soluble phosphorescent iridium complex as turn-on sensing material for human serum albumin

Chao Huang, Guoxia Ran, Yuan Zhao, Chan Wang and Qijun Song*

Key Laboratory of Synthetic and Biological Colloids, Ministry of Education, School of Chemical and Material Engineering, Jiangnan University, Wuxi 214122, P.R.China

* E-mail: qsong@jiangnan.edu.cn

The NMR spectrum of "Ir"

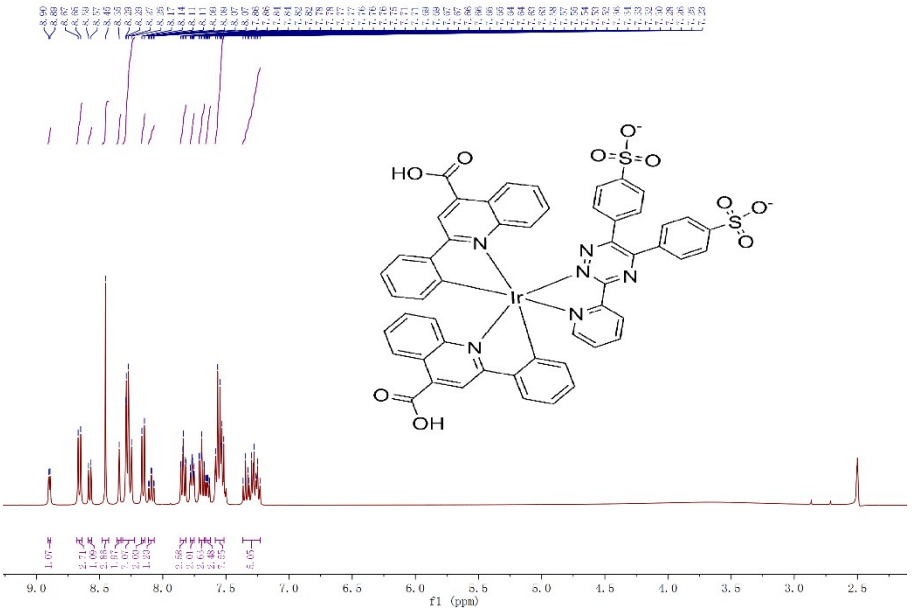

Fig. S1.H^1-NMR spectra of**Ir**

H^1-NMR (400 MHz, DMSO-d6), δ(ppm): 8.90 (d, J = 4.0 Hz, 1H), 8.66 (d, J = 8.0 Hz, 2H), 8.58 (d, J = 7.9 Hz, 1H), 8.45 (s, 2H), 8.32 – 8.22 (m, 4H), 8.16 (d, J = 8.2 Hz, 2H), 8.09 (td, J = 7.8, 1.7 Hz, 2H), 7.86 – 7.82 (m, 2H), 7.77 (ddt, J = 4.9, 3.5, 1.4 Hz, 2H), 7.71 – 7.67 (m, 2H), 7.58 – 7.52 (m, 4H), 7.37 – 7.23 (m, 6H).

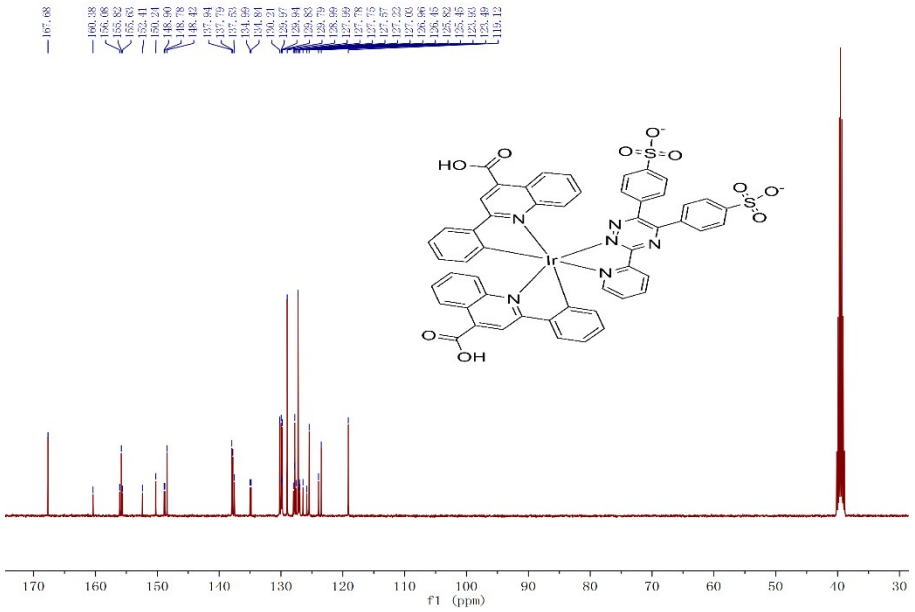

Fig. S2.C^{13}-NMR spectra of**Ir**

C^{13}-NMR (101 MHz, DMSO), δ(ppm):167.68, 160.38, 156.08, 155.82, 155.63, 152.41, 150.24, 148.90, 148.78, 148.42, 137.94, 137.79, 137.53, 134.99, 134.84, 130.21, 129.97, 129.94, 129.83, 129.79, 128.99, 127.99, 127.78, 127.75, 127.57, 127.22, 127.03, 126.96, 126.45, 125.82, 125.45, 123.93, 123.49, 119.12.

Density functional theory (DFT) calculation

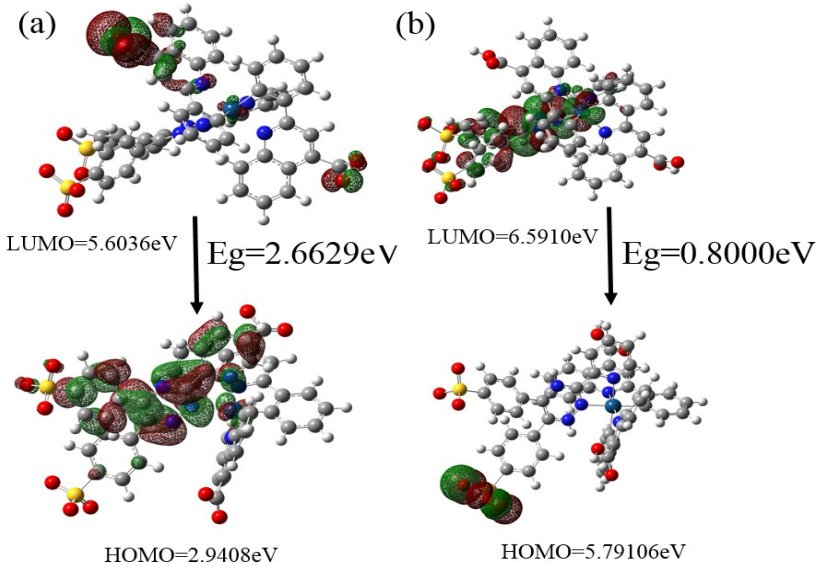

Fig.S3. The HOMO level and LUMO level of **Ir**in basic solution (a) and in acidic solution (b).

pKa of Ir

We can use the followingequilibrium from the literature[1] to describe the relationshipbetween the pH value and the phosphorescence intensity at λ_{ex}=338 nm quantitatively.

$$pKa = pH - log\left[\frac{I_{max} - I_x}{I_x - I_{min}}\right] \quad (3)$$

In the equilibrium, I_{min} and I_{max}represent thephosphorescence intensity of the probe in its acid andconjugate base, respectively. In Fig.S4, In wedescribedthelinearregressionrelationshipequilibrium (3) andpHvaluewiththefunctionof I =0.16473pH-0.2857 and R^2 = 0.9941.According to the equation in the literature[2, 3], we calculate that pKa1 and pKa2 is 2.51 and 3.23 whichstems from carboxylic acid. Similarly, pKa3and pKa4 is calculated to be 4.60 and 6.02 which belongs to ammonium ion.

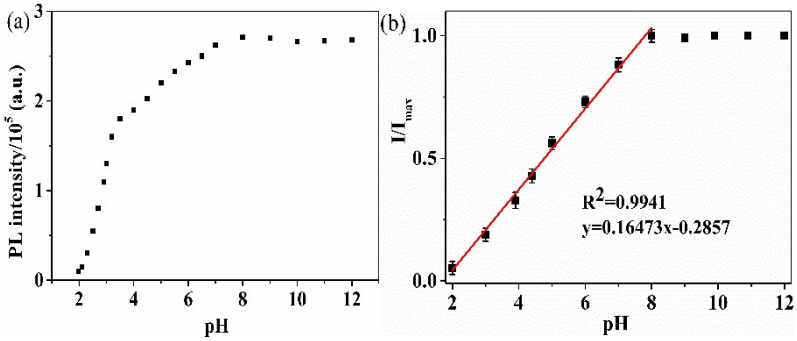

Fig. S4 (a) PL intensityat 634 nmversus pH, λ_{ex}=338nm. (b) The linear relationship of the phosphorescence intensity with pH value.

pH response

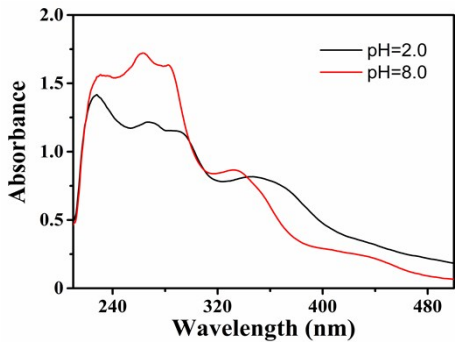

Fig. S5. The pH effect on the phosphorescence intensity ratio of d $I_{Ir\cdot HSA}/I_{Ir}$in BR solution.

Phosphorescence turn-on detection of Ir • HSA

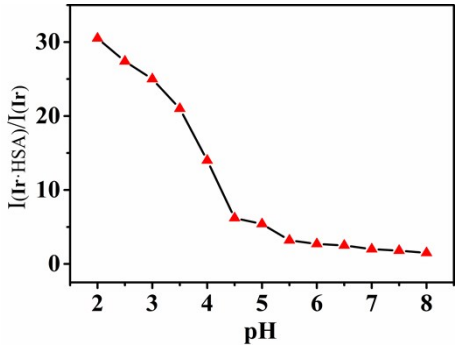

Fig. S6. The pH effect on the phosphorescence intensity ratio of d $I_{\mathbf{Ir}\cdot HSA}/I_{\mathbf{Ir}}$in BR solution.

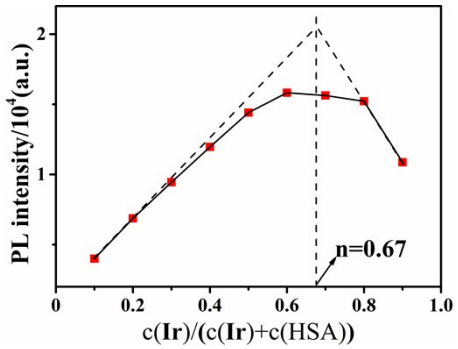

Fig. S7. Job's plots of phosphorescence intensities as functions of the molar fraction of HSA in BR solution at pH 2.0. The total concentration c(HSA) + c(**Ir**) iskept constant at 10 μM. The inflection points of job's plot give a value of 0.67, which correspond to the stoichiometric ratioof n(**Ir** : HSA) = 2:1. Excitation is performed at 338 nm.

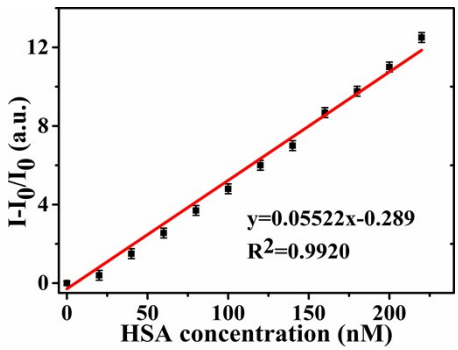

Fig.S8. The linear relationship of the phosphorescence intensity with HSA

concentration of 0-280nM (Error bars, SD, n=3), Conditions: in BR buffer (pH=2.0 0.04M), λ_{ex}=338 nm.

The interference study

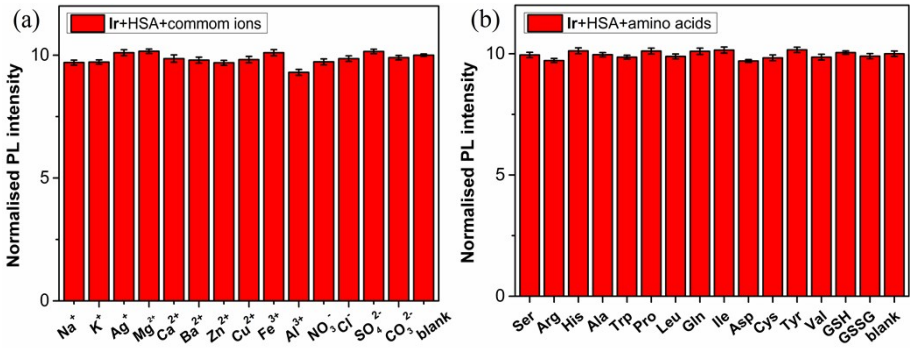

Fig. S9. Phosphorescence responses of **Ir** to HSA (blank, 10 μM) in the presence of (a) different metal ions: Na^+, K^+, Zn^{2+}, Mg^{2+},Ca^{2+}, Ba^{2+}, Al^{3+}, Cl^-, NO_3^-, SO_4^{2-}, CO_3^{2-}(10mM), Ag^+, Fe^{3+}, Cu^{2+} (1mM) and (b) amino acids (10 mM). Amino acids including Ser, Arg, His, Ala, Trp, Pro, Leu, Gln, Ile, Asp,Cys, Tyr, Val, GSH, GSSG. λex = 338 nm (Error bars, SD, n=3).

Table S1 The binding constants for **Ir** ·HSA through nonlinear fitting.

Compound	Stoichiometry	Temp (K)	K_1 (10^4M^{-1})	K_2 (10^4M^{-1})
Ir ·HSA	2:1	283	32.5	2.5
		293	29.9	2.2
		313	20.9	1.1

Table S2. Thermodynamic parameters of **Ir** ·HSA at 283K, 293K, 313K.

compound	Temp (K)	ΔG_1(kJ/mol)	ΔH_1 (kJ/mol)	ΔS_1 (J/K mol)	ΔG_2(kJ/mol)	ΔH_2 (kJ/mol)	ΔS_2 (J/K mol)
Ir ·HSA	283	-24.3	-16.5	27.6	-23.8	-10.5	47.0
	293	-25.3	-15.1	34.8	-24.4	-10.5	47.4
	313	-28.0	-10.2	56.9	-24.2	-12.6	37.1

[a]ln K =-ΔH/RT + constant; ΔG=-RT lnK; ΔG=ΔH-TΔS.

Real sample analysis

Table S3. Determination of HSA in real blood serum samples and urine samples.

Real Sample	This method		The clinical data	
	Found (mg ml^{-1})	RSD (%)[b]	Found(mg ml^{-1})[c]	RSD(%)[b]
Serum 1	23.7	2.3	23.5	2.3
Serum 1	40.3	2.0	40.1	2.0
Serum 1	50.9	1.8	51.3	1.8
Urine 1	10.5[a]	1.6	10.0[a]	1.7
Urine 2	53.0[a]	2.4	52.5[a]	2.0
Urine 3	218.1[a]	2.8	216.6[a]	2.3

a: μg ml^{-1}; b: relative standard deviation (n=5); c: The data got from hospital.

Table S4. Comparison of different methods for HSA detection.

methods	Linear range	Detection limit	Reference
Albumin-probe and host molecule	10-30 μM	0.5 μM	4
CuInZnS quantum dots-Co^{2+}	0.075 -100μM	45nM	5
Zero Current Potentiometry	30-363 nM	30nM	6
Dye Nanoparticles Fluorescence Sensor	3 -3000 nM	3 nM	7
Organic fluorescent probe DH1	0-3μM	83nM	8
Organic fluorescent probe AL-1	0-1 μM	6 nM	9
Iridium complex Phosphorescent probe	1-280nM	0.8nM	Present work

References:

1. X. Zhang, G.-J. Song, X.-J. Cao, J.-T. Liu, M.-Y. Chen, X.-Q. Cao and B.-X. Zhao, *Rsc Advances*, 2015, 5, 89827-89832.
2. M. Parambath, Q. S. Hanley, F. J. Martin-Martinez, T. Giesa, M. J. Buehler and C. C. Perry, *Physical Chemistry Chemical Physics*, 2016, 18, 5938-5948.
3. A. Lobnik, I. Oehme, I. Murkovic and O. S. Wolfbeis, *Analytica Chimica Acta*, 1998, 367, 159-165.
4. D. Patra, *Biosensors and Bioelectronics*, 2010, 25, 1149-1154.
5. W. Y. Gui, X. Q. Chen and Q. Ma, *Analytical and Bioanalytical Chemistry*, 2017, 409, 3871-3876.
6. H. Wang, Y. Wu and J.-F. Song, *Biosensors and Bioelectronics*, 2015, 72, 225-229.
7. P. Anees, S. Sreejith and A. Ajayaghosh, *Journal of the American Chemical Society*, 2014, 136, 13233-13239.
8. J. Fan, W. Sun, Z. Wang, X. Peng, Y. Li and J. Cao, *Chemical Communications*, 2014, 50, 9573-9576.
9. Y.-Y. Wu, W.-T. Yu, T.-C. Hou, T.-K. Liu, C.-L. Huang, I. C. Chen and K.-T. Tan, *Chemical Communications*, 2014, 50, 11507-11510.